Hindawi
Advances in Condensed Matter Physics
Volume 2018, Article ID 3175068, 13 pages
https://doi.org/10.1155/2018/3175068

Research Article

Acoustic Signatures of the Phases and Phase Transitions in the Blume Capel Model with Random Crystal Field

Gul Gulpinar

Department of Physics, Dokuz Eylül University, 35160 Izmir, Turkey

Correspondence should be addressed to Gul Gulpinar; gul.gulpinar@deu.edu.tr

Received 5 April 2018; Accepted 8 May 2018; Published 11 June 2018

Academic Editor: Oleg Derzhko

Sound propagation in the Blume Capel model with quenched diluted single-ion anisotropy is investigated. The sound dispersion relation and an expression for the ultrasonic attenuation are derived with the aid of the method of thermodynamics of irreversible processes. A frequency-dependent dispersion minimum that is shifted to lower temperatures with rising frequency is observed in the ordered region. The thermal and sound frequency (ω) dependencies of the sound attenuation and effect of the Onsager rate coefficient are studied in low- and high-frequency regimes. The results showed that $\omega\tau \ll 1$ and $\omega\tau \gg 1$ are the conditions that describe low- and high-frequency regimes, where τ is the single relaxation time diverging in the vicinity of the critical temperature. In addition, assuming a linear coupling of sound wave with the order parameter fluctuations in the system and ε as the temperature distance from the critical point, we found that the sound attenuation follows the power laws $\alpha(\omega, \varepsilon) \sim \omega^2\varepsilon^{-1}$ and $\alpha(\omega, \varepsilon) \sim \omega^0\varepsilon^1$ in the low- and high-frequency regions, while $\varepsilon \to 0$. Finally, a comparison of the findings of this study with previous theoretical and experimental studies is presented and it is shown that a good agreement is found with our results.

1. Introduction

The attenuation studies of acoustic waves in the vicinity of a magnetic ordering transition points provide insight into the critical dynamics of spin systems. Resonant ultrasound spectroscopy study of CoF_2 has shown the existence of a peak in sound attenuation as the Néel point is approached [1]. Magnetic phase diagram of multiferroic $MnWO_4$ has been obtained by sound velocity and attenuation measurements [2]. Investigation of the critical dynamics of sound propagation near continuous phase transition points not only provides valuable information about phase change mechanisms but also enables the determination of the critical indices that characterize these transitions [3]. Investigation of nonequilibrium processes probed by ultrasound waves in the spin-ice materials such as $Yb_2Ti_2O_7$ and $Dy_2Ti_2O_7$ [4, 5] and the frequency-dependent anisotropy of sound velocity and attenuation of the acoustic wave propagation through the nematic liquid crystals [6–8] represent examples to studies that are related to ultrasonic propagation in systems that undergo phase transitions. Further, considerable attention has been focused on the investigation of sound attenuation in disordered conductors [9]: the behavior of sound propagation near the λ point of the confined liquid ^{4}He [10–13] and absorption of ultrasound near the critical mixing point of a binary liquid [14–16]. Finally, one should note that a great variety of magnetic materials including halides, metals, oxides, intermetallics, and sulphides exhibit anomalies in their elastic properties due to the fact that order-disorder transitions are typically accompanied by small lattice distortions [17].

The Blume Capel (BC) model formulated independently by Blume [18] and Capel [19] plays a fundamental role in the multicritical phenomena associated with various physical systems, such as liquid crystals [20, 21], metallic alloys [22], proteins [23], and polymeric systems [24, 25]. On the other hand, the introduction of randomness changes the critical behaviors of a spin model considerably; that is, random fields can altogether eliminate the phase transitions in low dimensions and affect the numerical values of the critical exponents in higher dimensions [26–28]. Since then investigation of the effect of crystal field disorder on the

equilibrium phase diagram of spin-1 Ising models has been a research interest for many authors. The BC model with random single-ion anisotropy provides a microscopic model for phase transitions of ^{3}He-^{4}He mixtures in silica aerogel [29, 30] and relevant to the study of the phase separation in porous media in the vicinity of the superfluid transition [31, 32]. The interplay between quenched disorder provided by a random field and network connectivity in the BC model is investigated by using the replica method [33]. Moreover, the BC model with infinite-range ferromagnetic interactions and under the influence of a quenched disorder has been investigated and a classification of the phase diagrams in terms of their topology is presented in [34].

In this study, we investigate the critical dynamics of sound wave propagation in the BC model with bimodal crystal field by combining the statistical equilibrium theory and the thermodynamics of linear irreversible processes. This approach has been utilized to investigate the sound propagation in a great variety of model systems. Making use of the lowest approximation of the cluster variation method and linear response theory of irreversible processes, Erdem and Keskin performed the calculations of the sound attenuation near the critical point in the Blume-Emery-Griffiths (BEG) model with zero crystal field [35–37]. Gulpinar investigated the critical behavior of ultrasound wave absorption coefficient in the metamagnetic Ising model within the mean-field approximation [38]. Later, the absorption of sound in the spin-3/2 Ising model on the Bethe lattice is obtained and its temperature variance is analyzed near the phase transition points [39]. Recently, Cengiz and Albayrak studied the sound attenuation phenomena for a finite crystal field BEG model on the Bethe lattice in terms of the recursion relations by using the Onsager theory [40]. Due to mathematical complexity, the properties of critical sound propagation have not been studied in any spin system with random bond, random magnetic field, or random crystal field terms in the Hamiltonian expression. To the best of our knowledge, the critical dynamics of the sound propagation of the BC model with quenched diluted single-ion anisotropy have not been studied by the methods of irreversible thermodynamics. It is assumed in this manuscript that the sound wave is coupled to the order parameter fluctuations that decay mainly via order parameter relaxation process and the steady-state dynamics of the BC model with random diluted crystal field are formulated, while the system is under the effect of a propagating sound wave of frequency ω, which let us obtain the sound dispersion relation and sound attenuation coefficient for all temperatures and frequencies that contain effectively only one phenomenological rate coefficient. Temperature variance of sound dispersion and absorption has been investigated in the vicinity of the critical point. Finally, the frequency behavior of the attenuation coefficient for temperatures is presented in the vicinity of second-order transition from ordered to disordered phase.

The paper is organized as follows: the model and its static properties are presented briefly in Section 2. Next, the free energy production near the equilibrium is stated and the order parameter relaxation time is obtained in Section 3. The steady solution of the kinetic equation of the order parameter and expressions for the sound dispersion relation and ultrasonic attenuation coefficient are obtained in Section 4. Finally, frequency and temperature behaviors of the ultrasonic attenuation are analyzed and the discussion of the results is given in Section 5.

2. The Model and Its Equilibrium Properties

The BC model with random single-ion anisotropy in the presence of an external magnetic field H is described by the Hamiltonian

$$\widehat{H} = -J\sum_{\langle i,j\rangle}\sigma_i\sigma_j - H\sum_i\sigma_i + \sum_i\Delta_i\sigma_i^2, \tag{1}$$

with $\sigma_i = -1, 0, 1$. Here $J > 0$ is the exchange interaction due to ferromagnetic coupling and Δ_i is the crystal field acting on site i with a distribution function:

$$F(\Delta_i) = p\delta(\Delta_i - D) + (1-p)\delta(\Delta_i), \tag{2}$$

where p is concentration of the spins on the lattice which are influenced by a crystal field. The mean-field free energy for a nonvanishing external field is given by the following expression [41, 42]:

$$\begin{aligned}\Psi = {} & \Psi_0(V(a), T) + \frac{NzJ}{2}m^2 \\ & + NT\int \ln\left(1 - \frac{2\cosh((Jzm+H)/T)}{2\cosh((Jzm+H)/T) + e^{\Delta_i/T}}\right)F(\Delta_i)\,d\Delta_i,\end{aligned} \tag{3}$$

where $\Psi_0(V(a), T)$ is the lattice-free energy that is independent of spin configuration. Here a, V, and $m =< \sigma_i >$ are the lattice constant, volume, and order parameter of the system, respectively. In addition, $< \ldots >$ denotes thermal expectation value. If one makes use of (2), the mean-field free energy becomes

$$\begin{aligned}\Psi = {} & \Psi_0(V(a), T) + NzJ\frac{m^2}{2} + Np\Delta \\ & - pNk_BT\ln\left(2\cosh\frac{Jzm+H}{T} + e^{\Delta/T}\right) \\ & + (1-p)Nk_BT\ln\left(2\cosh\frac{Jzm+H}{T} + 1\right).\end{aligned} \tag{4}$$

For the sake of simplicity, we will take Boltzmann constant as unity ($k_B = 1$) from now on. The equilibrium conditions $(\partial\Psi/\partial m)|_{eq} = 0$ and $(\partial\Psi/\partial a)|_{eq} = 0$ give the following self-consistent equations for the magnetization and the lattice constant:

$$m = 2p\frac{\sinh\left(\left(Jzm+H\right)/T\right)}{2\cosh\left(\left(Jzm+H\right)/T\right)+e^{\Delta/T}} + 2\left(1-p\right) \cdot \frac{\sinh\left(\left(Jzm+H\right)/T\right)}{2\cosh\left(\left(Jzm+H\right)/T\right)+1}, \tag{5}$$

$$\left.\frac{\partial\Psi_0}{\partial a}\right|_{eq} = Nz\frac{\partial J}{\partial a}\left[-\frac{m^2}{2} + 2pzm\frac{\sinh\left(\left(Jzm+H\right)/T\right)}{2\cosh\left(\left(Jzm+H\right)/T\right)+e^{\Delta/T}} + 2\left(1-p\right)zm\frac{\sinh\left(\left(Jzm+H\right)/T\right)}{2\cosh\left(\left(Jzm+H\right)/T\right)+1}\right]. \tag{6}$$

The numerical solutions of the equation state given by (5) for vanishing external field have been performed and it has been reported that the BC model with quenched diluted single-ion anisotropy exhibits three distinct phase diagram topologies in the (T, Δ) plane depending on p [43, 44]. For $1 \geq p > 0.945$, the form of the phase diagram is identical to that of the pure BC model with homogenous crystal field, where the ferromagnetic phase is separated from the paramagnetic phase by a phase boundary that is of second order up to a tricritical point (TCP) at which the transition becomes first order. For $0.945 > p \geq 0.926$, TCP still exists but $\lambda-$ and first-order lines have reentrant parts. The phase diagram of the system changes dramatically in nature if one increases the dilutence further: For $0.926 > p \geq 8/9$, there exists discontinuous phase transitions between the ferromagnetic and paramagnetic phases at strong crystal fields and low temperatures. The transition becomes continuous at higher temperatures. Further, the λ-line displays reentrance. A portion of the second-order transition line is masked by a first-order transition line. This situation causes two distinct multicritical points to appear: critical endpoint (CEP) and double critical endpoint (DCP). Under a threshold value of the crystal field concentration ($p \leq 8/9$), the quenched disorder completely eliminates the first-order phase transitions, and the whole phase boundary is of second order.

3. Relaxation Dynamics of the BC Model with Quenched Diluted Single-Ion Anisotropy

One may assume the existence of a small uniform external field for a short while in order to be able to formulate the relaxation dynamics of the BC model with random single-ion anisotropy. In addition, the amplitude of the external field should be sufficiently small to allow the spin system to be in the neighborhood of equilibrium, where linear response theory can be utilized. In other words, we investigate the final stage of the approach to equilibrium. In the case of the existence of a small deviation of the magnetic field from its equilibrium value $\delta H = H - H_0$, the system will be removed slightly from equilibrium and a finite free energy production $\Delta\Psi$ will arise:

$$\Delta\Psi = \Psi\left(m, H, a\right) - \Psi_0\left(m_0, H_0, a_0\right), \tag{7}$$

where $\Delta\Psi$ corresponds to an increase in the corresponding thermodynamic potential related to the deviation of m, a, H from their equilibrium values and Ψ_0 is the equilibrium value of the free energy, while $m = m_0$, $a = a_0$, and $H = H_0$. In the neighborhood of equilibrium, the free energy production may be written as a Taylor-series expansion, in which deviations in the thermodynamic quantities are retained to second order:

$$\Delta\Psi = \frac{A}{2}\left(m-m_0\right)^2 - B\left(m-m_0\right)\left(H-H_0\right) + \frac{C}{2}\left(H-H_0\right)^2 + D\left(m-m_0\right)\left(a-a_0\right) + E\left(a-a_0\right)\left(H-H_0\right) + \frac{F}{2}\left(a-a_0\right)^2 + G\left(H-H_0\right). \tag{8}$$

Here, the coefficients A to G are the so-called free energy production coefficients and they are calculated by the following second-order derivatives:

$$\begin{aligned}
A &= \left.\frac{\partial^2\Psi}{\partial m^2}\right|_{eq},\\
B &= -\left.\frac{\partial^2\Psi}{\partial m\partial H}\right|_{eq},\\
C &= \left.\frac{\partial^2\Psi}{\partial H^2}\right|_{eq},\\
D &= \left.\frac{\partial^2\Psi}{\partial m\partial a}\right|_{eq} = \left.\frac{\partial^2\Psi}{\partial m\partial J}\right|_{eq}\left.\frac{\partial J}{\partial a}\right|_{eq},\\
E &= \left.\frac{\partial^2\Psi}{\partial H\partial a}\right|_{eq} = \left.\frac{\partial^2\Psi}{\partial H\partial J}\right|_{eq}\left.\frac{\partial J}{\partial a}\right|_{eq},\\
F &= \left.\frac{\partial^2\Psi}{\partial a^2}\right|_{eq}\\
&= \left.\frac{\partial^2\Psi_0}{\partial a^2}\right|_{eq} + \left.\frac{\partial^2\Psi}{\partial J^2}\right|_{eq}\left(\left.\frac{\partial J}{\partial a}\right|_{eq}\right)^2 + \left.\frac{\partial\Psi}{\partial J}\right|_{eq}\left.\frac{\partial^2 J}{\partial a^2}\right|_{eq},\\
G &= \left.\frac{\partial\Psi}{\partial H}\right|_{eq},
\end{aligned} \tag{9}$$

where the subscript "eq" denotes the thermal equilibrium; thus the derivatives are evaluated for $m = m_0$, $a = a_0$, and $H = H_0$. The explicit expressions for the above-mentioned free energy production coefficients are given in the Appendix.

If the system is shifted from its equilibrium by the deviation of the external field from its equilibrium value ($\delta H \neq 0$) and/or by the volume change of the crystal which is proportional to $a - a_0$, the generalized force X_m arises, which can be regarded as the force that brings magnetization back to its equilibrium value. The generalized force conjugate to

generalized current may be obtained by differentiating the free energy production with respect to $(m - m_0)$:

$$X_m = -\frac{\partial \Delta\Psi}{\partial (m - m_0)} = -\left[A(m - m_0) - B(H - H_0) + D(a - a_0)\right]. \quad (10)$$

In the realm of theory of irreversible thermodynamics, the time derivative of magnetization $(\dot{m})$ is treated as the generalized current conjugate to X_m:

$$\dot{m} = \frac{d(m - m_0)}{dt}. \quad (11)$$

If the deviation from the equilibrium condition is small, one can write a linear relation between the current and the force: $\dot{m} = LX_m$. Thus, the dynamics of the order parameter for the BC model with quenched diluted crystal field are ruled by the following rate equation:

$$\dot{m} = -L\left[A(m - m_0) - B(H - H_0) + D(a - a_0)\right], \quad (12)$$

where L is the order parameter Onsager coefficient. We should note that, in this study, the most simple temperature dependence is assumed for L, which must be found either in principle by a more powerful theory such as path probability method [45, 46] or in practice by fit with the experimental findings.

For the case of vanishing external stimulation ($H = H_0$, $a = a_0$), one obtains the relation that describes the rate of change in the order parameter relaxing to its equilibrium state as follows:

$$\dot{m} = -LA(m - m_0). \quad (13)$$

The solution of the kinetic equation given by (13) is of the form $(m - m_0 \simeq e^{-t/\tau})$, where τ is the relaxation time of the order parameter. Thus, the relaxation time corresponds to

$$\tau = \frac{1}{LA}. \quad (14)$$

The temperature behavior of the order parameter relaxation time near the phase transition points of the BC model with bimodal crystal field has been investigated in detail in [44] and a rapid increase in the single relaxation time is observed when the temperature approaches the critical and multicritical phase transition temperatures. In addition, τ presents a scaling relation $\tau \sim |T - T_C|^{-1}$, which corresponds to well-known phenomena of critical slowing down. Finally, as a signature of the first-order phase transition, a jump-discontinuity has been observed in the relaxation time near a first-order phase transition.

4. Derivation of the Sound Attenuation Coefficient

In this section, we will study the transport properties for the BC model with bimodal crystal field near its magnetic phase transition points. With this aim, we will consider the case in which the lattice is stimulated by the sound wave of frequency ω. Due to nature of the linear response theory, if you perturb the system at a frequency ω, the response will take place at same frequency. Thus, one can find the steady-state solution of (12) with an oscillating external force $a - a_0 = a_1 e^{i\omega t}$ as follows:

$$m - m_0 = m_1 e^{i\omega t}. \quad (15)$$

Introduce this expression into (12).

And assuming that $H = H_0$, one obtains the following nonhomogenous equation for m_1:

$$i\omega m_1 e^{i\omega t} = -LAm_1 e^{i\omega t} - LDa_1 e^{i\omega t}. \quad (16)$$

Solving (16) for m_1/a_1 gives

$$\frac{m_1}{a_1} = -\frac{LD}{i\omega + LA}. \quad (17)$$

In addition, if one makes use of (14) for the relaxation time of the BC model with a random crystal field, (17) becomes

$$\frac{m_1}{a_1} = -\frac{LD\tau}{1 + i\omega\tau}. \quad (18)$$

The response in the pressure $p - p_0$ is obtained by differentiating the minimum work with respect to $V - V_0$:

$$p - p_0 = \frac{\partial \Delta\Psi}{\partial (V - V_0)} = -\frac{a}{3V_0}\frac{\partial \Delta\Psi}{\partial (a - a_0)}. \quad (19)$$

Then, using (8), one obtains

$$p - p_0 = -\frac{a_0}{3V_0}\left[D(m - m_0) + F(a - a_0)\right]. \quad (20)$$

On the other hand, the derivative of pressure with respect to volume gives

$$\left(\frac{\partial p}{\partial V}\right)_{sound} = -\frac{a_0^2}{9V_0^2}\left[D\frac{m_1}{a_1} + F\right], \quad (21)$$

where D and F are the free energy production coefficients that are given in (9). If one introduces (18) and the density $\rho = M/V_0$ into (21),

$$\left(\frac{\partial p}{\partial \rho}\right)_{sound} = \frac{a_0^2}{9M}\left[F - \frac{LD^2\tau}{1 + i\omega\tau}\right]. \quad (22)$$

Finally, using the definition $c_{sound} = (\partial p/\partial \rho)^{1/2}_{sound}$ and the fact that the order parameter relaxation time tends to very large values in the vicinity of the continuous phase transition points, one obtains the complex effective elastic constant (complex velocity of sound) of the BC model with quenched diluted crystal field:

$$c_{sound} \cong \frac{a_0}{3}\sqrt{\frac{F}{M}}\left[1 - \frac{LD^2\tau}{2F(1 + i\omega\tau)}\right]. \quad (23)$$

It is a well-known fact that the lag between the oscillations of the pressure and the excitation of a given mode leads to the dissipation of energy and dispersion of the sound wave.

$$c(\omega) = \mathrm{Re}\{c_{sound}\} = \frac{a_0}{3\sqrt{M}}\sqrt{F}\frac{2F - LD^2\tau}{2F\left(1+\omega^2\tau^2\right)}. \tag{24}$$

Since we assume a linear coupling of sound wave with the order parameter fluctuations in the system, the dispersion which is the relative sound velocity change with frequency depends not on the sound wave amplitude but on frequency ω. Finally, if one makes use of the following definition for the sound attenuation constant,

$$\begin{aligned}\alpha(\omega) &= \mathrm{Im}\left\{\frac{-\omega}{c_{sound}}\right\} \\ &= \mathrm{Im}\left\{\left(\frac{a_0}{3}\sqrt{\frac{F}{M}}\right)^{-1}\left[\frac{-2\omega F(1+i\omega\tau)}{2F - LD^2\tau + i2F\omega\tau}\right]\right\}, \\ &= \frac{3\sqrt{M}}{2a_0}\frac{1}{\left(\sqrt{F}\right)^3}\frac{LD^2\omega^2\tau^2}{\left(1-\dfrac{LD^2\tau}{2F}\right)+\omega^2\tau^2}.\end{aligned} \tag{25}$$

A finite attenuation above the critical temperature cannot be obtained due to the fact that the attenuation constant is proportional to free energy production constant D that vanishes above the critical temperature, where the order parameter is equal to zero (see (A.1)). This is entirely due to the mean-field approximation and one may expect a finite attenuation constant above the critical temperature for higher-order approximations (i.e., Bethe approximation).

Now, if one rewrites the free-energy production coefficient F given in (9), the following expressions are obtained for $\sqrt{F}$ and $(\sqrt{F})^{-3}$:

$$\begin{aligned}\sqrt{F} \simeq \sqrt{\left.\frac{\partial^2\Psi_0}{\partial a^2}\right|_{eq}}&\left\{1+\frac{1}{2}\left(\left.\frac{\partial^2\Psi_0}{\partial a^2}\right|_{eq}\right)^{-1}\right. \\ &\left.\cdot\left[\left.\frac{\partial^2\Psi}{\partial J^2}\right|_{eq}\left(\left.\frac{\partial J}{\partial a}\right|_{eq}\right)^2+\left.\frac{\partial\Psi}{\partial J}\right|_{eq}\left.\frac{\partial^2 J}{\partial a^2}\right|_{eq}\right]\right\},\end{aligned} \tag{26}$$

$$\begin{aligned}\left(\sqrt{F}\right)^{-3} \simeq \left(\left.\frac{\partial^2\Psi_0}{\partial a^2}\right|_{eq}\right)^{-3/2}&\left\{1-\frac{3}{2}\left(\left.\frac{\partial^2\Psi_0}{\partial a^2}\right|_{eq}\right)^{-1}\right. \\ &\left.\cdot\left[\left.\frac{\partial^2\Psi}{\partial J^2}\right|_{eq}\left(\left.\frac{\partial J}{\partial a}\right|_{eq}\right)^2+\left.\frac{\partial\Psi}{\partial J}\right|_{eq}\left.\frac{\partial^2 J}{\partial a^2}\right|_{eq}\right]\right\}.\end{aligned} \tag{27}$$

In addition, if one uses the definition $c_\infty^2 = (a_0^2/9M)(\partial^2\Psi_0/\partial a^2)|_{eq}$, (24) and (25) become

$$\begin{aligned}c(\omega) = c_\infty&\left\{1+\frac{1}{2}\left(\left.\frac{\partial^2\Psi_0}{\partial a^2}\right|_{eq}\right)^{-1}\right. \\ &\left.\cdot\left[\left.\frac{\partial^2\Psi}{\partial J^2}\right|_{eq}\left(\left.\frac{\partial J}{\partial a}\right|_{eq}\right)^2+\left.\frac{\partial\Psi}{\partial J}\right|_{eq}\left.\frac{\partial^2 J}{\partial a^2}\right|_{eq}\right]\right\} \\ &\cdot\frac{2F - LD^2\tau}{2F\left(1+\omega^2\tau^2\right)},\end{aligned} \tag{28}$$

$$\begin{aligned}\alpha(\omega) = \frac{a_0^2}{18M}\frac{1}{c_\infty^3}&\left\{1-\frac{3}{2}\left(\left.\frac{\partial^2\Psi_0}{\partial a^2}\right|_{eq}\right)^{-1}\right. \\ &\left.\cdot\left[\left.\frac{\partial^2\Psi}{\partial J^2}\right|_{eq}\left(\left.\frac{\partial J}{\partial a}\right|_{eq}\right)^2+\left.\frac{\partial\Psi}{\partial J}\right|_{eq}\left.\frac{\partial^2 J}{\partial a^2}\right|_{eq}\right]\right\} \\ &\cdot\frac{LD^2\omega^2\tau^2}{\left(1-LD^2\tau/2F\right)+\omega^2\tau^2},\end{aligned} \tag{29}$$

where c_∞ is the velocity of sound for very high frequencies at which order parameter can no longer follow the sound wave motion.

5. Results And Discussion

The calculated data that provides information about the thermal variation of the sound velocity and attenuation coefficient in the ordered and disordered phases and the frequency dependence of isothermal attenuation coefficient in the ordered phase of the BC model with quenched diluted crystal field will be discussed in the following. In addition, the behavior of sound absorption in the neighborhood of critical temperature is analyzed according to various values of phenomenological rate coefficient. Finally, by making use of double logarithmic plots of the sound attenuation coefficient versus the distance from the critical temperature, the dynamical critical exponents of the sound absorption are obtained for low- and high-frequency regimes. Before starting to discuss the above-mentioned results, it is convenient to introduce the following reduced quantities:

$$\begin{aligned}\theta &= \frac{T}{zJ}, \\ d &= \frac{D}{zJ}, \\ h &= \frac{H}{zJ};\end{aligned} \tag{30}$$

here, θ, d, and h are the reduced values of the temperature, crystal field, and magnetic field, respectively. One should stress that we focus on zero field case ($h = 0.0$) and c_∞^3 is taken as unity for the sake of simplicity throughout this section.

Figure 1 displays the temperature variation of the frequency-dependent sound velocity (dispersion) of the BC model with quenched diluted crystal field for several values of sound wave frequency, while $L = 0.02$, $p = 0.98$,

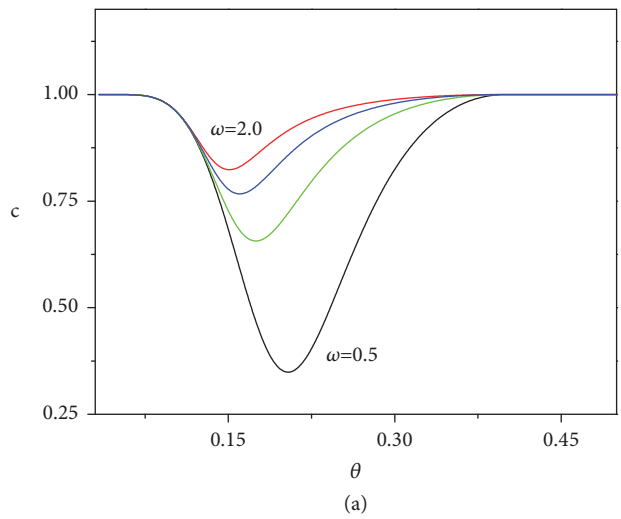

FIGURE 1: Sound dispersion at different frequencies of sound for $L = 0.02$, $p = 0.98$, and $d = d_C = 0.45$. The number accompanying each curve represents the value of the sound frequency ω.

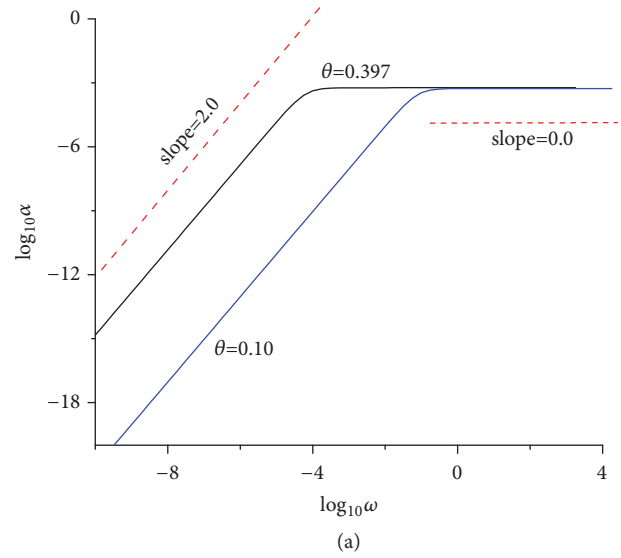

FIGURE 2: Double logarithmic plot of attenuation versus frequency for $L = 0.02$, $p = 0.98$, $d = d_C = 0.45$, and $\theta_C = 0.39747$. The number accompanying each curve represents the value of the reduced temperature.

and $d = 0.45$. The number accompanying each curve denotes the value of ω and one observes a characteristic sound velocity minimum that shifts to the lower temperatures with increasing frequency. The minima become deeper with decreasing ω and ultrasonic dispersion reaches the finite value of 1.0 at $\theta = \theta_C$ and remains temperature-independent after then. Similar temperature dependence of the sound dispersion has been reported near the order-disorder phase transition point of the BEG model [47]. Comparably, the existence of the minima of the sound velocity in the ordered phase and its shift to lower temperatures with increasing frequency have been observed in the classical liquid crystals [8], liquid ^{4}He confined in a microfluidic cavity [10], and the magnetic compound $RbMnF_3$ [48]. In addition, it can be seen from Figure 1 that the change in sound velocity becomes frequency-independent as one approaches to critical value of the reduced temperature and this behavior is in parallel with the findings of the molecular field theory [17, 49], dynamical renormalization group theory for the propagation of sound near the continuous structural phase transitions [50], and Brillouin scattering studies of A_2MX_6-crystals [49].

Figure 2 illustrates the double logarithmic plot of the isothermal α versus ω for two distinct values of the reduced temperature ($\theta = 0.10, 0.390 < \theta_C$) in the ferromagnetic phase, while $p = 0.98$, $L = 0.02$, $\theta_C = 0.39747$, and $d_C = 0.45$. One can observe the usual ω^2 dependence of the attenuation in the low-frequency region, where $\omega\tau << 1$. This result is in accordance with the theoretical and experimental findings for CoF_2 [1] and MnF_2 [51, 52]. The ultrasonic attenuation has different frequency dependence in the high-frequency regime at which order parameter can no longer follow sound wave motion: this part of the plot has zero slope; thus, ultrasonic attenuation behaves as $\alpha \propto \omega^0$, while $\omega\tau >> 1$. In addition, there is a crossover behavior in attenuation between low- and high-frequency regimes. The theoretical treatment of the sound propagation by mode-mode coupling method predicts that the sound attenuation coefficient scales as $\alpha \sim \omega^y$ for the sound frequencies that are quite larger than the characteristic frequency of the order parameter fluctuations ω_c and an extensive study of the frequency dispersion of the critical attenuation of $KMnF_3$ above 186.2 K measured $y = 0.13 \pm 0.05$ [53–55]. In addition, similar frequency dependence of the sound attenuation coefficient has been reported for various model systems such as spin-1 and spin-3/2 Ising models on the Bethe lattice [39, 40], zero crystal field BEG model [37], and metamagnetic Ising model [38] within mean-field theory.

Figures 3(a)-3(c) show the calculated sound attenuation coefficient as a function of the reduced temperature θ near the critical point for various values of the sound frequency whose value is denoted by the number accompanying each curve and the vertical dashed lines refer to critical temperature θ_c, while $p = 0.98$, $L = 0.02$, and $d = 0.45$. One can observe from these figures that the attenuation rises to a maximum in the ordered phase for all values of ω. But the frequency dependencies of the location form and amplitude of the absorption peak is different for low- and high-frequency regions. Figure 3(a) presents the temperature variance of α for two values of the sound frequency $\omega = 1.2 \times 10^{-5}, \omega = 1.8 \times 10^{-5}$ (blue and red curves), which satisfy the condition $\omega\tau \ll 1$ for the low-frequency regime. In the low-frequency region, the sound attenuation peak is rather sharp and located very near to the critical temperature θ_c and its amplitude increases with rising sound frequency.

Figure 3(b) presents the temperature dependence of α for higher values of the sound frequency ($\omega = 0.002, 0.005, 0.2, 0.5, 1.0$). It is observed from this figure that the absorption peak is rather broad and its amplitude grows with rising frequency for these ranges of the frequency. Further, the temperature at which attenuation maxima take

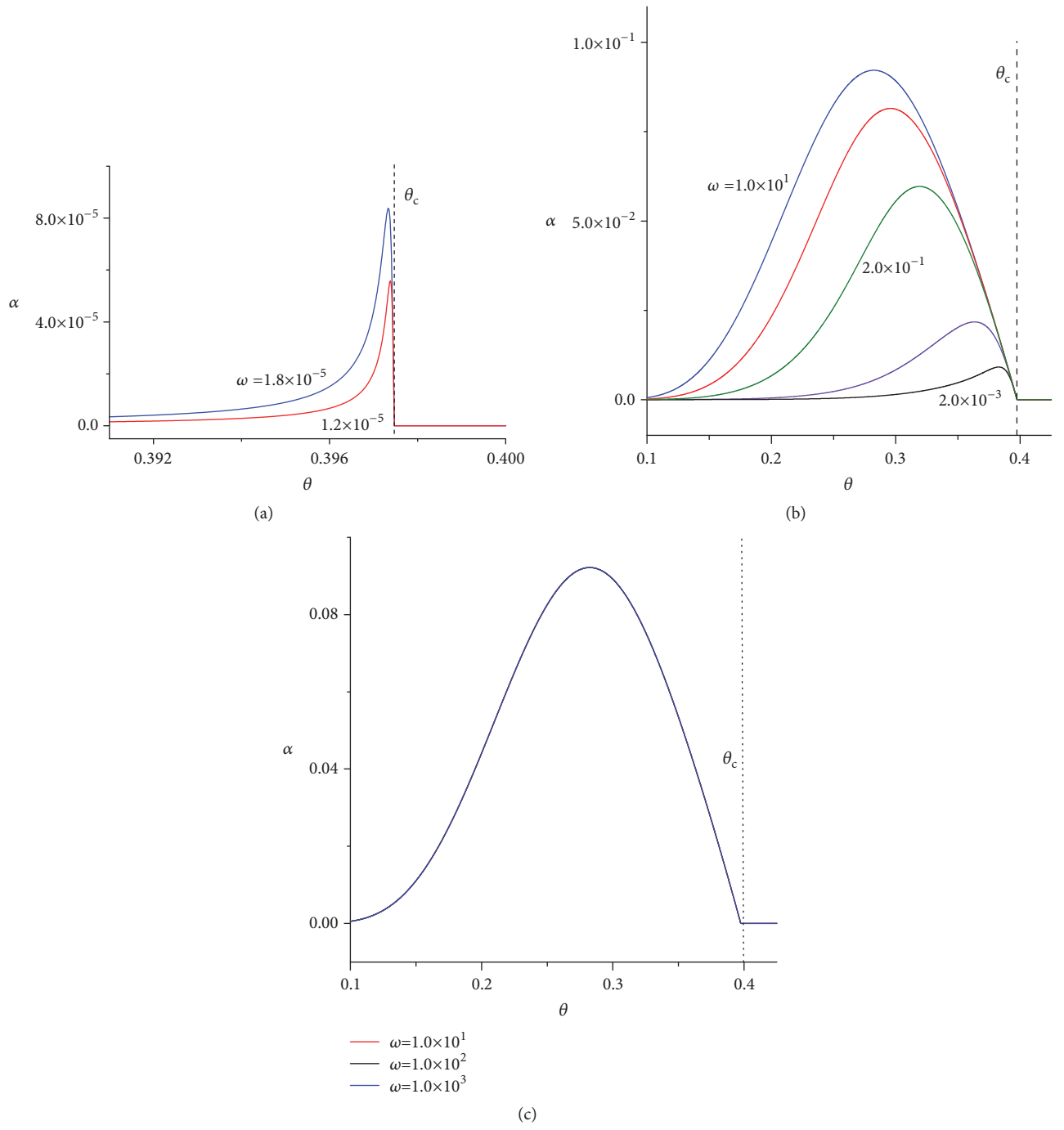

FIGURE 3: Sound attenuation α as a function of the reduced temperature at several sound frequency values ω in the neighborhood of a critical point for $p = 0.98$, $d = d_C = 0.45$, and $L = 0.02$. The number accompanying each curve denotes the value of the frequency ω and the vertical dotted line represents the critical temperature in the ordered phase.

place moves to lower temperatures with rising frequency. The frequency shift of the attenuation maxima is also observed in the experimental and theoretical studies of the ultrasonic investigation of liquid helium [56, 57] and Rb_2ZnCl_4 and K_2SeO_4 [58] as well as other Ising models [37–40] and elastically isotropic Ising system above the critical point on the basis of a complete stochastic model [59].

In Figure 3(c), we aim to illustrate the temperature dependence of the sound attenuation coefficient for three distinct values of the sound frequency ($\omega = 1, 10, 1000$) for which $\omega\tau >> 1$ and the order parameter can no longer follow sound wave motion. Both the location and the amplitude of the absorption peak do not change with the sound frequency and this is in accordance with the power law $\alpha \sim \omega^0$ observed

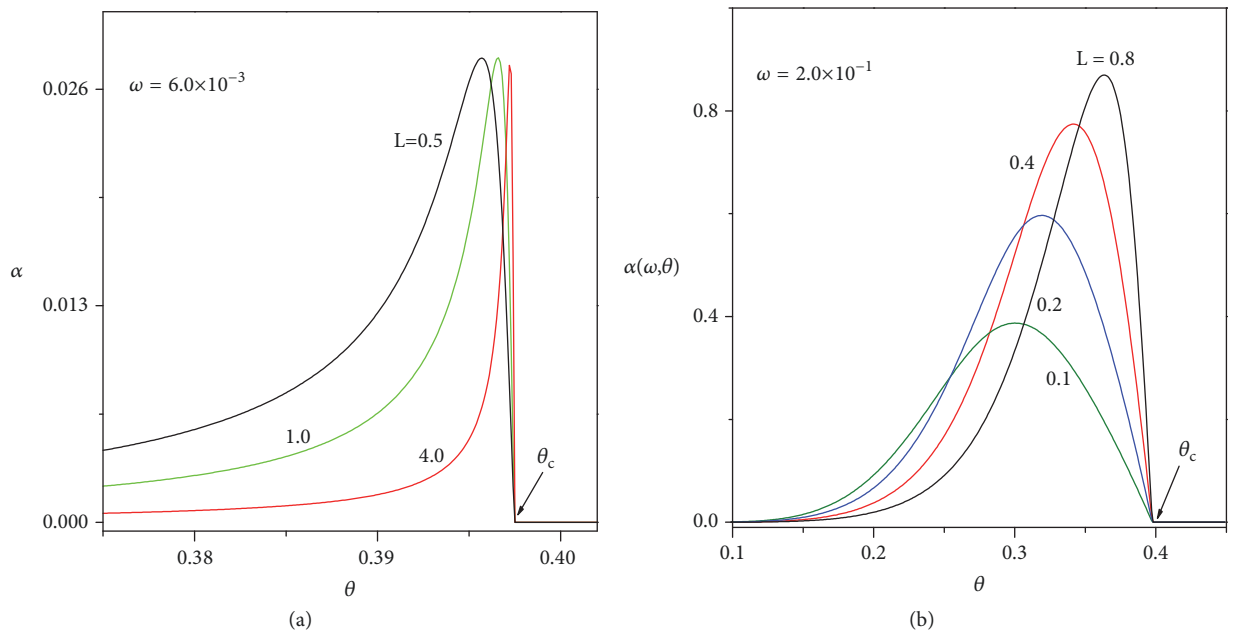

FIGURE 4: Ultrasonic attenuation as a function of reduced temperature for (a) $\omega = 0.006$ and (b) $\omega = 0.2$ while $p = 0.98$ and $d = d_C = 0.45$. The number accompanying each curve denotes the value of the order parameter Onsager coefficient (L) and the arrow denotes the critical temperature.

in Figure 2, while $\omega\tau >> 1$. Similar results are observed for metamagnetic Ising and BEG models in the high-frequency region. But since these models have two order parameters and their relaxation dynamics are governed by two relaxation times, their attenuation coefficient have two peaks for some frequency values in the low-frequency region as expected [37, 38].

It is clear from (14) and (28) that both the single relaxation time and sound attenuation coefficient depend on the phenomenological Onsager rate coefficient (L). Detailed investigation of the relaxation dynamics of the BC model with bimodal random crystal field revealed the fact that the relaxation time increases and the order parameter relaxation slows down with rising L [44]. Due to fact that thermal fluctuations become very large and the correlation distance extends over large number of spins, the coupling between sound waves and order parameter relaxation gives rise to an increase in the absorption of the sound waves as the temperature approaches its critical value. As the transition temperature of a solid is closely approached, the ordered parameter relaxes slow enough; the internal irreversible processes that tend to restore local equilibrium are switched on and they make the entropy increase, which results in energy dissipation in the system [17, 57]. Due to these facts, we found it interesting to study the effect of L on the temperature variance of the sound attenuation near the second-order phase transition point. Figures 4(a) and 4(b) illustrate the attenuation coefficient versus reduced temperature at several values of L for $p = 0.98$ and $d = 0.45$ at two distinct values of the sound wave frequency ω and the arrows refer to critical point temperature. It is apparent from Figure 4(a) which displays the calculated α for $\omega = 0.006$ that the maxima of α broaden and move to lower temperatures with decreasing L. Meanwhile the value of the sound attenuation maxima slightly increases with decreasing L. The attenuation peak broadens and its amplitude decreases and shifts to lower temperatures with decreasing L, while $\omega = 0.2$. We should note that, for systems that have two or more order parameters, the relation between the generalized forces and currents may be written in terms of a matrix of phenomenological rate coefficients and the effect of the nondiagonal Onsager coefficient has been investigated for BEG and metamagnetic Ising models in the mean-field approximation [37, 38] and spin-3/2 and spin-1 Ising models on the Bethe lattice [39, 40].

The critical behavior of the sound attenuation coefficient in the neighborhood of the second-order phase transition points is characterized by the dynamical sound attenuation critical exponent ρ. As discussed above, isothermal sound attenuation coefficient behaves as $\alpha \propto \omega^2$ for frequencies that satisfy the condition $\omega\tau << 1$ and $\alpha \propto \omega^0$ for $\omega\tau >> 1$. In addition, the comparison of Figures 3(a)–3(c) reveals the fact that the constant frequency temperature variance of α near the critical temperature is different in low- and high-frequency regions. Consequently, one may expect two distinct power law relations and two distinct exponents (ρ_l, ρ_h) for these two regions:

$$\alpha(\omega, \varepsilon) \approx \begin{cases} \omega^2 \varepsilon^{-\rho_l} & \text{for } \omega\tau \ll 1, \\ \omega^0 \varepsilon^{-\rho_h} & \text{for } \omega\tau \gg 1, \end{cases} \tag{31}$$

where $\varepsilon = \theta - \theta_C$ is the expansion parameter, which is a measure of the distance from the critical temperature.

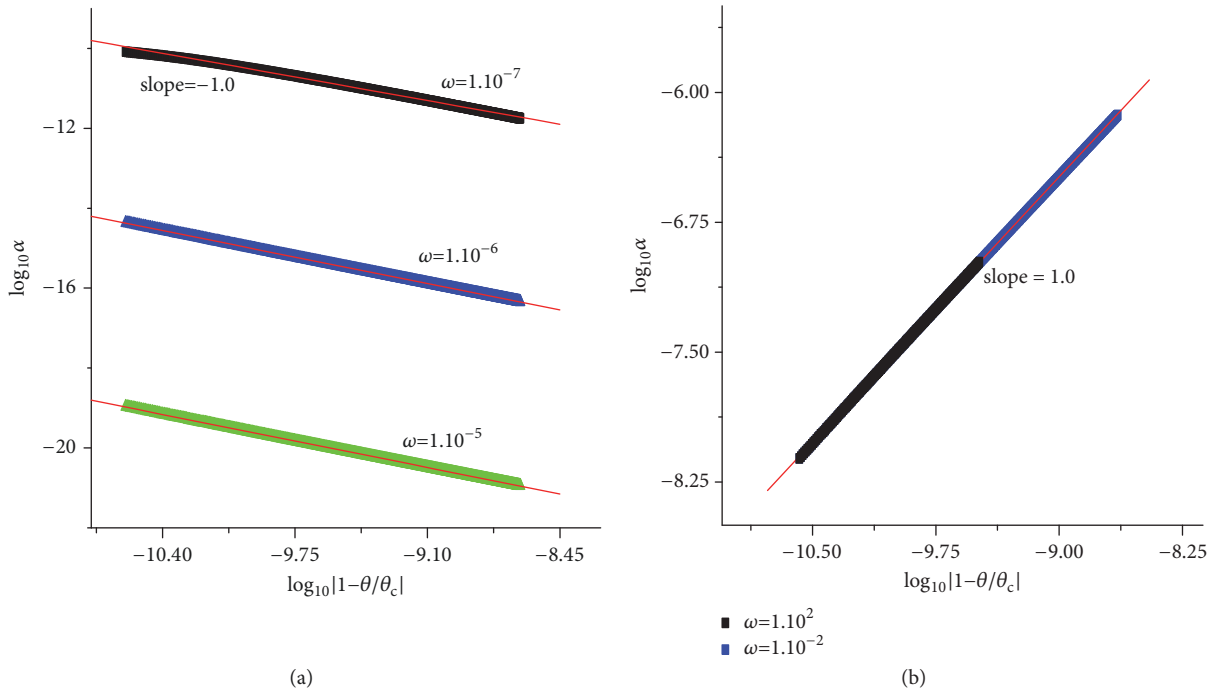

FIGURE 5: Double logarithmic plots of attenuation versus $|1-\theta/\theta_C|$ for (a) low-frequency and (b) high-frequency regimes in the neighborhood of a critical point for $p = 0.98$, $d = d_C = 0.45$, and $L = 0.02$.

The critical exponents for the function $\alpha(\omega, \varepsilon)$ are defined, respectively, as

$$\rho_l = -\lim_{\varepsilon \to 0} \frac{\ln |\alpha(\omega, \varepsilon)|}{\ln |\varepsilon|} \quad \text{for } \omega\tau \ll 1,$$
$$\rho_h = -\lim_{\varepsilon \to 0} \frac{\ln |\alpha(\omega, \varepsilon)|}{\ln |\varepsilon|} \quad \text{for } \omega\tau \gg 1. \tag{32}$$

In order to calculate the values of these exponents, one may sketch log – log plots of the sound attenuation coefficient versus $|1-\theta/\theta_C|$ and find the slopes of the linear parts of these curves, which will be equal to $-\rho_l$ and $-\rho_h$ for frequencies that satisfy the conditions $\omega\tau \ll 1$ and $\omega\tau \gg 1$, respectively. With this aim, Figures 5(a) and 5(b) illustrate the $\log_{10}\alpha - \log_{10}|1 - \theta/\theta_C|$ plots for the constant values of sound frequencies in low- and high-frequency regions, respectively. Figure 5(a) displays three distinct curves for $\omega = 1.0 \times 10^{-7}$ (black curve), $\omega = 1.0 \times 10^{-6}$ (blue curve), and $\omega = 1.0 \times 10^{-5}$ (green curve), which obey the $\omega\tau \ll 1$ condition. As one can see from this figure, for all three frequencies in the low-frequency region, the slopes of the linear part of $\log_{10}\alpha - \log_{10}|1 - \theta/\theta_C|$ curves are equal to −1; namely, $\rho_l = 1$. Utilizing (31) and (30), one obtains the power law $\alpha(\omega, \varepsilon) \sim \omega^2\varepsilon^{-1}$ of the sound attenuation coefficient for the BC model with bimodal random crystal field in the low-frequency regime. This result is in accordance with the scaling behavior of the sound attenuation coefficient α_{LK} obtained within the Landau-Khalatnikov theory, which applies to bilinear, quadratic coupling of strain-order parameter coupling [17, 57]: $\alpha_{LK} \sim \omega^2\tau$ and the order parameter relaxation time behaves as $\tau \sim \varepsilon^{-1}$ as $\varepsilon \to 0$ within the mean-field approximation [44]. A strong anomalous increase of the sound attenuation as the temperature approaches its critical value has been also observed for systems that undergo (elastic and distortive) structural phase transitions. The dynamical renormalization group calculations for distortive structural phase transitions report $\rho_\sigma = (z\nu + \alpha_\sigma)$, where $\alpha_\sigma = \alpha + 2(\phi - 1)(1 - \delta_{\sigma,1})$, where z, ν, ϕ, and are α are the dynamical, correlation length, heat capacity, and crossover critical exponents, respectively. Utilizing the same method, Schwabl showed that the sound attenuation coefficient scales as $\alpha \sim \varepsilon^{-3/2}\omega^2$ in the vicinity of the critical point of the elastic structural phase transitions [50]. Ultrasonic measurements reported small but positive attenuation exponents in isotropic garnet structured magnets such as $Y_3Fe_5O_{12}$ and $Gd_3Fe_5O_{12}$ [60]. Recently, resonant ultrasound spectroscopy studies of CoF_2 have shown that $\rho = 0.9$ to 1.1 for the resonance peaks near 487, 860, 1300 and 1882 kHz, which depend strongly on the shear modulus [1].

Finally, Figure 5(b) shows the linear part of the $\log\alpha$ versus $\log|1 - \theta/\theta_C|$ curves for frequencies $\omega = 0.1$ (blue symbols) and $\omega = 100$ (black symbols), while $\omega\tau \gg 1$. One can see from this figure that the slope of the curves is +1; thus $\rho_h = -1$. If one again makes use of (30) and (31), the following power law can be written for the sound absorption: $\alpha(\omega, \varepsilon) \sim \omega^0\varepsilon^1$, while $\omega\tau \gg 1$ and verifies the convergence of the sound absorption to zero as the reduced temperature approaches its critical value (see Figure 3(b)). We should note that similar behavior is observed in the high-frequency region of the sound attenuation for the BEG model [37]. It has been shown by the phenomenological theory that sound attenuation reaches the saturation value $\alpha_{phe} \to B\tau^{-1}$ for very

high frequencies, where B is independent of temperature and frequency for a system with a single relaxation process [3]. If one keeps in mind that $\tau \sim \varepsilon^{-1}$ as $\varepsilon \to 0$, this corresponds to $\alpha_{phe}(\omega, \varepsilon) \approx \omega^0 \varepsilon^1$, which is in parallel with our result.

6. Concluding Remarks

The present study is devoted to critical dynamics of sound propagation in BC model with a random single anisotropy by using a method that combines the statistical equilibrium theory of phase transitions with the linear response theory of irreversible thermodynamics. With this aim, it is supposed that the system is stimulated by a sound wave oscillating at an angular frequency ω and the complex effective elastic constant and sound velocity and sound attenuation coefficient are obtained for all temperatures and frequencies by studying the steady-state solutions. We have studied the temperature behavior of the sound velocity for various values of the sound frequency and observed a characteristic minimum that shifts to the lower temperatures with rising frequency and a frequency-independent sound velocity in the vicinity of critical temperature. Then, we have investigated the temperature, frequency, and order parameter Onsager rate coefficient dependencies of the sound attenuation near the second transition temperatures. Frequency-dependent shifts in attenuation maxima to lower temperatures with increasing frequency for temperatures less than the second-order phase transition temperatures are obtained and possible mechanisms for these phenomena are discussed. Our investigation of the frequency variance of the isothermal sound attenuation revealed the fact that sound attenuation follows the power law $\alpha \sim \omega^2$ for frequencies that satisfy the condition $\omega\tau \ll 1$ and $\alpha \sim \omega^0$, while $\omega\tau \gg 1$. Consequently, $\omega\tau$ is the quantity that determines the separation of the low- and high-frequency regimes. By making use of this information and obtaining the slope of the $\log\alpha$ versus $\log|1 - \theta/\theta_c|$ plots, we have obtained that sound absorption follows the scaling relation $\alpha(\omega, \varepsilon) \sim \omega^2 \varepsilon^{-1}$ in the low-frequency regime and the power law $\alpha(\omega, \varepsilon) \sim \omega^0 \varepsilon^1$ for frequencies that obey the condition $\omega\tau \gg 1$. Finally, we should note that the high-frequency behavior provides information about the damping mechanism.

In this study, the sound attenuation related to the relaxation process of the order parameter for BC model with a random single anisotropy is studied. We would like to emphasize that the above-mentioned theory is limited neither to the systems with only scalar spin nor to the magnetic phase transitions. It could also apply to a crystalline solid and other systems whenever the order parameter dynamics are relaxation dynamics. We should note that there are additional possible reasons for attenuation peaks in magnetic systems which are not taken into account in the current analysis, such as coupling of the sound waves to modes, domain effects, and nuclear acoustic resonance [17]. In addition, in the case of real crystals with many structural defects, the presence of disorder will affect the critical behavior of the sound attenuation in solid media. The field-theoretic description of dynamic critical effects of the disorder on acoustic anomalies near the temperature of second-order phase transition for three-dimensional Ising-like systems has shown that the presence of impurities brings additional couplings changing the value of the critical exponent of the sound attenuation and strongly affects the order parameter shape function at the low-frequency region in the vicinity of the critical point [61].

Appendix

The free energy production coefficients A to G that are defined in (9) are given as follows:

$$A = NJz - \frac{NJ^2z^2}{T}\left[\frac{2p\cosh\left(Jzm_0/T\right)}{2\cosh\left(Jzm_0/T\right)+e^{\Delta/T}} - \left(\frac{2\sqrt{p}\sinh\left(Jzm_0/T\right)}{2\cosh\left(Jzm_0/T\right)+e^{\Delta/T}}\right)^2 + \frac{2\left(1-p\right)\cosh\left(Jzm_0/T\right)}{2\cosh\left(Jzm_0/T\right)+1} - \left(\frac{2\sqrt{1-p}\sinh\left(Jzm_0/T\right)}{2\cosh\left(Jzm_0/T\right)+1}\right)^2\right],$$

$$B = \frac{NJz}{T}\left[\frac{2p\cosh\left(Jzm_0/T\right)}{2\cosh\left(Jzm_0/T\right)+e^{\Delta/T}} - \left(\frac{2\sqrt{p}\sinh\left(Jzm_0/T\right)}{2\cosh\left(Jzm_0/T\right)+e^{\Delta/T}}\right)^2 + \frac{2\left(1-p\right)\cosh\left(Jzm_0/T\right)}{2\cosh\left(Jzm_0/T\right)+1} - \left(\frac{2\sqrt{1-p}\sinh\left(Jzm_0/T\right)}{2\cosh\left(Jzm_0/T\right)+1}\right)^2\right],$$

$$C = -\frac{N}{T}\left[\frac{2p\cosh\left(Jzm_0/T\right)}{2\cosh\left(Jzm_0/T\right)+e^{\Delta/T}} - \left(\frac{2\sqrt{p}\sinh\left(Jzm_0/T\right)}{2\cosh\left(Jzm_0/T\right)+e^{\Delta/T}}\right)^2 + \frac{2\left(1-p\right)\cosh\left(Jzm_0/T\right)}{2\cosh\left(Jzm_0/T\right)+1} - \left(\frac{2\sqrt{1-p}\sinh\left(Jzm_0/T\right)}{2\cosh\left(Jzm_0/T\right)+e^{\Delta/T}}\right)^2\right],$$

$$D = Nz\left.\frac{\partial J}{\partial a}\right|_{eq}\left[m_0 - \frac{2Jzm_0p\cosh\left(Jzm_0/T\right)}{T\left[2\cosh\left(Jzm_0/T\right)+e^{\Delta/T}\right]} - \frac{2p\sinh\left(Jzm_0/T\right)}{2\cosh\left(Jzm_0/T\right)+e^{\Delta/T}}\right.$$

$$+\frac{4Jzm_0p\sinh^2\left(Jzm_0/T\right)}{T\left[2\cosh\left(Jzm_0/T\right)+e^{\Delta/T}\right]^2}$$
$$-\frac{2Jzm_0\left(1-p\right)\cosh\left(Jzm_0/T\right)}{T\left[2\cosh\left(Jzm_0/T\right)+1\right]}$$
$$-\frac{2\left(1-p\right)\sinh\left(Jzm_0/T\right)}{2\cosh\left(Jzm_0/T\right)+1}$$
$$+\frac{4Jzm_0\left(1-p\right)\sinh^2\left(Jzm_0/T\right)}{T\left[2\cosh\left(Jzm_0/T\right)+1\right]}\Bigg],$$

$$E=-\frac{Nzm_0}{T}\left[\frac{2p\cosh\left(Jzm_0/T\right)}{2\cosh\left(Jzm_0/T\right)+e^{\Delta/T}}\right.$$
$$-\left(\frac{2\sqrt{p}\sinh\left(Jzm_0/T\right)}{2\cosh\left(Jzm_0/T\right)+e^{\Delta/T}}\right)^2$$
$$+\frac{2\left(1-p\right)\cosh\left(Jzm_0/T\right)}{2\cosh\left(Jzm_0/T\right)+1}$$
$$\left.-\left(\frac{2\sqrt{1-p}\sinh\left(Jzm_0/T\right)}{2\cosh\left(Jzm_0/T\right)+1}\right)^2\right],$$

$$F=\left.\frac{\partial^2\Psi_0}{\partial a^2}\right|_{eq}+Nzm_0\left.\frac{\partial^2 J}{\partial a^2}\right|_{eq}\left[\frac{m_0}{2}\right. \tag{A.1}$$
$$-\frac{2\left(1-p\right)\cosh\left(Jzm_0/T\right)}{2\cosh\left(Jzm_0/T\right)+1}$$
$$\left.-\frac{2p\cosh\left(Jzm_0/T\right)}{2\cosh\left(Jzm_0/T\right)+e^{\Delta/T}}\right]+\frac{Nz^2m_0^2}{T}\left(\left.\frac{\partial J}{\partial a}\right|_{eq}\right)^2$$
$$\times\left[\frac{2p\cosh\left(Jzm_0/T\right)}{2\cosh\left(Jzm_0/T\right)+e^{\Delta/T}}\right.$$
$$-\left(\frac{2\sqrt{p}\sinh\left(Jzm_0/T\right)}{2\cosh\left(Jzm_0/T\right)+e^{\Delta/T}}\right)^2$$
$$+\frac{2\left(1-p\right)\cosh\left(Jzm_0/T\right)}{2\cosh\left(Jzm_0/T\right)+1}$$
$$\left.-\left(\frac{2\sqrt{1-p}\sinh\left(Jzm_0/T\right)}{2\cosh\left(Jzm_0/T\right)+1}\right)^2\right],$$

$$G=\frac{2N\left(1-p\right)\cosh\left(Jzm_0/T\right)}{2\cosh\left(Jzm_0/T\right)+1}$$
$$-\frac{2Np\sinh\left(Jzm_0/T\right)}{2\cosh\left(Jzm_0/T\right)+e^{\Delta/T}}.$$

Data Availability

The data that support the findings of this study are available from the corresponding author upon reasonable request.

Disclosure

The research and publication of this article was performed as a part of the employment of the author, Department of Physics, Dokuz Eylül University, Department of Physics, İzmir, Turkey.

Conflicts of Interest

The author declares that there are no conflicts of interest.

References

[1] R. I. Thomson, T. Chatterji, and M. A. Carpenter, "CoF_2: A model system for magnetoelastic coupling and elastic softening mechanisms associated with paramagnetic ↔ antiferromagnetic phase transitions," *Journal of Physics: Condensed Matter*, vol. 26, no. 14, Article ID 146001, 2014.

[2] V. Felea, P. Lemmens, S. Yasin et al., "Magnetic phase diagram of multiferroic $MnWO_4$ probed by ultrasound," *Journal of Physics: Condensed Matter*, vol. 23, no. 21, Article ID 216001, 2011.

[3] A. Pawlak, "Critical sound propagation in magnets," in *Horizons in World Physics*, L. Pedroza and M. Everett, Eds., vol. 268, pp. 1–69, Nova Science Publishers, Hauppauge, NY, USA, 2009.

[4] S. Bhattacharjee, S. Erfanifam, E. L. Green et al., " Acoustic signatures of the phases and phase transitions in ," *Physical Review B: Condensed Matter and Materials Physics*, vol. 93, no. 14, 2016.

[5] S. Erfanifam, S. Zherlitsyn, J. Wosnitza et al., "Intrinsic and extrinsic nonstationary field-driven processes in the spin-ice compound $Dy_2Ti_2O_7$," *Physical Review B: Condensed Matter and Materials Physics*, vol. 84, no. 22, Article ID 220404, 2011.

[6] S. S. Turzi, "Viscoelastic nematodynamics," *Physical Review E: Statistical, Nonlinear, and Soft Matter Physics*, vol. 94, no. 6, Article ID 062705, 2016.

[7] P. Biscari, A. DiCarlo, and S. S. Turzi, "Anisotropic wave propagation in nematic liquid crystals," *Soft Matter*, vol. 10, no. 41, pp. 8296–8307, 2014.

[8] C. Grammes, J. K. Krüger, K.-P. Bohn et al., "Universal relaxation behavior of classical liquid crystals at hypersonic frequencies," *Physical Review E: Statistical, Nonlinear, and Soft Matter Physics*, vol. 51, no. 1, pp. 430–440, 1995.

[9] A. Shtyk and M. Feigel'Man, "Ultrasonic attenuation via energy diffusion channel in disordered conductors," *Physical Review B: Condensed Matter and Materials Physics*, vol. 92, no. 19, Article ID 195101, 2015.

[10] X. Rojas, B. D. Hauer, A. J. MacDonald, P. Saberi, Y. Yang, and J. P. Davis, " Ultrasonic interferometer for first-sound measurements of confined liquid ," *Physical Review B: Condensed Matter and Materials Physics*, vol. 89, no. 17, 2014.

[11] E. Krotscheck and M. D. Miller, "Third sound and stability of thin ^{3}He-^{4}He films," *Physical Review B*, vol. 73, article 134514, pp. 1–14, 2006.

[12] J. M. Valles, R. M. Heinrichs, and R. B. Hallock, " ^{3}He-^{4}He Mixture Films: The He coverage dependence of the ^{3}He binding energy," *Physical Review Letters*, vol. 56, pp. 1704–1707, 1986.

[13] P. A. Sheldon and R. B. Hallock, "Third sound and energetics in," *Physical Review B: Condensed Matter and Materials Physics*, vol. 50, no. 21, pp. 16082–16085, 1994.

[14] D. B. Fenner, "Nonsingular absorption of ultrasound near the critical mixing point of a binary liquid," *Physical Review A:*

Atomic, Molecular and Optical Physics, vol. 23, no. 4, pp. 1931–1940, 1981.

[15] P. K. Khabibullaev, S. Z. Mirzaev, and U. Kaatze, "Critical fluctuations and noncritical relaxations of the nitrobenzene-isooctane system near its consolute point," *Chemical Physics Letters*, vol. 458, no. 1-3, pp. 76–80, 2008.

[16] S. Z. Mirzaev and U. Kaatze, "Scaling function of critical binary mixtures: Nitrobenzene-n-hexane data revisited," *Chemical Physics*, vol. 393, no. 1, pp. 129–134, 2012.

[17] B. Lüthi, *Physical Acoustics in the Solid State*, Springer, Berlin, Germany, 2005.

[18] M. Blume, "Theory of the first-order magnetic phase change in UO_2," *Physical Review A: Atomic, Molecular and Optical Physics*, vol. 141, no. 2, pp. 517–524, 1966.

[19] H. W. Capel, "On the possibility of first-order phase transitions in Ising systems of triplet ions with zero-field splitting," *Physica A: Statistical Mechanics and its Applications*, vol. 32, no. 5, pp. 966–988, 1966.

[20] P. E. Cladis, R. K. Bogardus, W. B. Daniels, and G. N. Taylor, "High-pressure investigation of the reentrant nematic - Bilayer-smectic-A transition," *Physical Review Letters*, vol. 39, no. 11, pp. 720–723, 1977.

[21] G. P. Johari, "The Tammann phase boundary, exothermic disordering and the entropy contribution change on phase transformation," *Physical Chemistry Chemical Physics*, vol. 3, no. 12, pp. 2483–2487, 2001.

[22] W. Sinkler, C. Michaelsen, R. Bormann, D. Spilsbury, and N. Cowlam, "Neutron-diffraction investigation of structural changes during inverse melting ofs," *Physical Review B: Condensed Matter and Materials Physics*, vol. 55, no. 5, pp. 2874–2881, 1997.

[23] M. I. Marqués, J. M. Borreguero, H. E. Stanley, and N. V. Dokholyan, "Possible mechanism for cold denaturation of proteins at high pressure," *Physical Review Letters*, vol. 91, no. 13, 2003.

[24] S. Rastogi, G. W. Höhne, and A. Keller, "Unusual Pressure-Induced Phase Behavior in Crystalline Poly(4-methylpentene-1): Calorimetric and Spectroscopic Results and Further Implications," *Macromolecules*, vol. 32, no. 26, pp. 8897–8909, 1999.

[25] A. L. Greer, "Too hot to melt," *Nature*, vol. 404, no. 6774, pp. 134-135, 2000.

[26] A. N. Berker, "Ordering under random fields: Renormalization-group arguments," *Physical Review B: Condensed Matter and Materials Physics*, vol. 29, no. 9, pp. 5243–5245, 1984.

[27] Y. Imry and S. Ma, "Random-field instability of the ordered state of continuous symmetry," *Physical Review Letters*, vol. 35, no. 21, pp. 1399–1401, 1975.

[28] G. Grinstein and S.-K. Ma, "Surface tension, roughening, and lower critical dimension in the random-field Ising model," *Physical Review B: Condensed Matter and Materials Physics*, vol. 28, no. 5, pp. 2588–2601, 1983.

[29] A. Falicov and A. N. Berker, "Correlated Random-Chemical-Potential Model for the Phase Transitions of Helium Mixtures in Porous Media," *Physical Review Letters*, vol. 74, no. 3, pp. 426–429, 1995.

[30] M. Paetkau and J. R. Beamish, "Tricritical point and superfluid transition in ^{3}He-^{4}He mixtures in silica aerogel," *Physical Review Letters*, vol. 80, no. 25, pp. 5591–5594, 1998.

[31] L. B. Lurio, N. Mulders, M. Paetkau, M. H. W. Chan, and S. G. J. Mochrie, "Small-angle x-ray scattering measurements of the microstructure of liquid helium mixtures adsorbed in aerogel," *Physical Review E: Statistical, Nonlinear, and Soft Matter Physics*, vol. 76, no. 1, Article ID 011506, 2007.

[32] T. R. Prisk, C. Pantalei, H. Kaiser, and P. E. Sokol, "Confinement-driven phase separation of quantum liquid mixtures," *Physical Review Letters*, vol. 109, no. 7, Article ID 075301, 2012.

[33] R. Erichsen, A. A. Lopes, and S. G. Magalhaes, "Multicritical points and topology-induced inverse transition in the random-field Blume-Capel model in a random network," *Physical Review E: Statistical, Nonlinear, and Soft Matter Physics*, vol. 95, no. 6, Article ID 062113, 2017.

[34] P. V. Santos, F. A. da Costa, and J. M. de Araujo, "Mean-field solution of the Blume-Capel model under a random crystal field," *Physics Letters A*, vol. 379, no. 22-23, pp. 1397–1401, 2015.

[35] M. Keskin and R. Erdem, "Critical behaviors of the sound attenuation in a spin-1 Ising model," *The Journal of Chemical Physics*, vol. 118, no. 13, pp. 5947–5954, 2003.

[36] R. Erdem and M. Keskin, "On the temperature dependence of the sound attenuation maximum as a function of frequency and magnetic field in a spin-1 Ising model near the critical region," *Physics Letters A*, vol. 326, no. 1-2, pp. 27–31, 2004.

[37] R. Erdem and M. Keskin, "Sound attenuation in a spin-1 ising system near the critical temperature," *Physics Letters A*, vol. 291, no. 2-3, pp. 159–164, 2001.

[38] G. Gulpinar, "Critical behavior of sound attenuation in a metamagnetic Ising system," *Physics Letters A*, vol. 372, no. 2, pp. 98–105, 2008.

[39] T. Cengiz and E. Albayrak, "The Bethe lattice treatment of sound attenuation for a spin- 3/2 Ising model," *Physica A: Statistical Mechanics and its Applications*, vol. 391, no. 10, pp. 2948–2956, 2012.

[40] T. Cengiz and E. Albayrak, "The crystal field effects on sound attenuation for a spin-1 Ising model on the Bethe lattice," *Journal of Statistical Mechanics: Theory and Experiment*, vol. 2012, no. 7, Article ID P07004, 2012.

[41] G. Gülpınar, R. Erdem, and M. Ağartıoğlu, "Critical and multi-critical behaviors of static and complex magnetic susceptibilities for the mean-field Blume-Capel model with a random crystal field," *Journal of Magnetism and Magnetic Materials*, vol. 439, pp. 44–52, 2017.

[42] G. Gulpinar and R. Erdem, "High-frequency magnetic field on crystal field diluted S=1 Ising system: Magnetic relaxation near continuous phase transition points," *Canadian Journal of Physics*, 2018.

[43] A. Benyoussef, M. Saber, T. Biaz, and M. Touzani, "The spin-1 Ising model with a random crystal field: The mean-field solution," *Journal of Physics C: Solid State Physics*, vol. 20, no. 32, pp. 5349–5354, 1987.

[44] G. Gulpinar and F. Iyikanat, "Dynamics of the Blume-Capel model with quenched diluted single-ion anisotropy in the neighborhood of equilibrium states," *Physical Review E: Statistical, Nonlinear, and Soft Matter Physics*, vol. 83, no. 4, Article ID 041101, 2011.

[45] R. Kikuchi, "The path probability method," *Progress of Theoretical Physics Supplement*, vol. 35, pp. 1–64, 1966.

[46] A. Erdinç and M. Keskin, "Equilibrium and nonequilibrium behavior of the Blume–Emery–Griffiths model using the pair approximation and path probability method with the pair distribution," *International Journal of Modern Physics B*, vol. 18, no. 10n11, pp. 1603–1626, 2004.

[47] R. Erdem and M. Keskin, "Sound dispersion in a spin-1 Ising system near the second-order phase transition point," *Physics Letters A*, vol. 310, no. 1, pp. 74–79, 2003.

[48] T. J. Moran and B. Lüthi, "High-frequency sound propagation near magnetic phase transitions," *Physical Review B: Condensed Matter and Materials Physics*, vol. 4, no. 1, pp. 122–132, 1971.

[49] W. Henkel, J. Pelzl, K. H. Höck, and H. Thomas, "Elastic constants and softening of acoustic modes in A_2MX_6-crystals observed by Brillouin scattering," *Zeitschrift für Physik B Condensed Matter and Quanta*, vol. 37, no. 4, pp. 321–332, 1980.

[50] F. Schwabl, "Propagation of sound at continuous structural phase transitions," *Journal of Statistical Physics*, vol. 39, no. 5-6, pp. 719–737, 1985.

[51] A. Ikushima, "Anisotropy of the ultrasonic attenuation in MnF_2 near the Néel temperature," *Journal of Physics and Chemistry of Solids*, vol. 31, no. 5, pp. 939–946, 1970.

[52] A. Pawlak, "Critical sound propagation in MnF_2," *Physica Status Solidi (c)*, vol. 3, pp. 204–207, 2006.

[53] K. Kawasaki, "Sound Attenuation and Dispersion near the Liquid-Gas Critical Point," *Physical Review A*, vol. 1, pp. 1750–1757, 1970.

[54] Y. Shiwa and K. Kawasaki, "The Mode-Coupling Approach to Sound Propagation in a Critical Fluid. I: – Correction Due to Hydrodynamic Interactions –," *Progress of Theoretical and Experimental Physics*, vol. 66, no. 1, pp. 118–128, 1981.

[55] M. Suzuki, "Dynamical scaling and ultrasonic attenuation in $KMnF_3$ at the structural phase transition," *Journal of Physics C: Solid State Physics*, vol. 13, no. 4, article no. 013, pp. 549–560, 1980.

[56] D. T. Sprague, N. Alikacem, P. A. Sheldon, and R. B. Hallock, " ^{3}He binding energy in thin helium-mixture films," *Physical Review Letters*, vol. 72, no. 3, pp. 384–387, 1994.

[57] L. D. Landau, I. M. Khalatnikov,"On the anomalous absorption of sound near a second-order phase transition point," Dokl. Akad. Nauk SSSR 96, 469 (1954), reprinted in "Collected Papers of L. D. Landau", Ed. D. Ter Haar, Pergamon, London, UK, 1965.

[58] A. M. Schorgg and F. Schwabl, "Theory of ultrasonic attenuation at incommensurate phase transitions," *Physical Review B: Condensed Matter and Materials Physics*, vol. 49, no. 17, pp. 11682–11703, 1994.

[59] A. Pawlak, "Theory of critical sound attenuation in Ising-type magnets," *Acta Physica Polonica A*, vol. 98, no. 1-2, pp. 23–39, 2000.

[60] I. K. Kamilov and K. K. Aliev, "Ultrasonic studies of the critical dynamics of magnetically ordered crystals," *Physics-Uspekhi*, vol. 41, no. 9, pp. 865–884, 1998.

[61] P. V. Prudnikov and V. V. Prudnikov, "Critical sound attenuation of three-dimensional lsing systems," *Condensed Matter Physics*, vol. 9, no. 2, pp. 403–410, 2006.